



Power Electronic Systems
Laboratory

© 2013 IEEE

Proceedings of the Brazilian Power Electronics Conference (COBEP 2013), Gramado, Brazil, October 27-31, 2013

Three-Phase Modular Multilevel Current Source Rectifiers for Electric Vehicle Battery Charging Systems

T. Soeiro,
M. Heldwein,
J. W. Kolar

This material is published in order to provide access to research results of the Power Electronic Systems Laboratory / D-ITET / ETH Zurich. Internal or personal use of this material is permitted. However, permission to reprint/republish this material for advertising or promotional purposes or for creating new collective works for resale or redistribution must be obtained from the copyright holder. By choosing to view this document, you agree to all provisions of the copyright laws protecting it.



Eidgenössische Technische Hochschule Zürich
Swiss Federal Institute of Technology Zurich

THREE-PHASE MODULAR MULTILEVEL CURRENT SOURCE RECTIFIERS FOR ELECTRIC VEHICLE BATTERY CHARGING SYSTEMS

Thiago B. Soeiro*, Marcelo L. Heldwein* and Johann W. Kolar†

*Federal University of Santa Catarina – UFSC / Power Electronics Institute - INEP
P.O. Box 5119, 88040-970 - Florianopolis, BRAZIL

†Swiss Federal Institute of Technology – ETH Zürich / Power Electronic Systems Laboratory
Physikstrasse 3 8092- Zürich, SWITZERLAND
Email: heldwein@inep.ufsc.br

Abstract— This paper discusses three-phase high power factor AC-to-DC current source converters appropriate for Electric Vehicle (EV) battery charging systems. The AC grid interfaces are multilevel current source rectifiers constructed from standard power electronic circuits that have their fast-switched semiconductors and output inductors replaced with several modular subcircuits connected in parallel. By operating the parallel circuits with an appropriate phase-shifted PWM, the systems feature low current and voltage ripples at the input and output terminals, allowing size reduction of the passive filters. In addition, as the DC-link current can be efficiently distributed to the modularized subcircuits, better efficiency, due to the lower conduction and switching losses, is achievable. The characteristics of the presented EV systems, including the principles of operation, modulation strategy, and feedback control are described. The feasibility of a remarkable solution, namely a three-phase five-level six-switch buck-type PFC is demonstrated by means of a constructed hardware prototype.

I. INTRODUCTION

Charging of Electric Vehicle (EV) batteries inherently requires conversion of energy from the AC mains into DC-quantities. Several charging voltage and power levels have been defined by different standardization organizations (IEC 61851, IEC62196, SAE J1772). Single-phase Power Factor Corrector (PFC) mains interfaces are commonly employed for low charging power levels, e.g. $P < 5$ kW, whereas for higher charging power levels, three-phase PFCs are used [1]. The EV charger, typically implemented as a two-stage system, i.e. comprising a PFC rectifier input stage followed by a DC-DC converter, can be either integrated into the car (on-board chargers) or accommodated in specially designed EV charging stations (off-board chargers) [2]. Basic requirements for such systems are controlled output voltage, high power factor, and high efficiency. If the power electronics have to be accommodated on-board the EV, low weight and high power density are also desirable [1]-[4]. Finally, if isolation of the PFC output from the DC-bus is necessary due to safety reasons, this could be provided by an isolated DC-DC converter. Possible power electronic configurations for charging of EVs are given in Fig. 1 [5].

With respect to public high power charging infrastructures, also called semi- or ultra-fast chargers, the nearly empty battery should be re-charged in the shortest time possible. These EV chargers, supplied from three-phase AC lines at 110/220 V (*rms*) and 50/60 Hz, typically require a peak power ranging from 10 kW to 150 kW in order to inject direct current into the battery sets at variable voltage levels according to the vehicle (50 V to 600 V) [6]. Buck-type three-phase PFC rectifiers, also known as Current Source Rectifiers (CSRs), are appropriate for these high power chargers as a direct connection to the battery could be used. Compared to the boost-type systems, buck-type topologies provide

a wider output voltage control range, while maintaining PFC capability at the input, and can potentially enable direct start-up, while allowing for dynamic current limitation [3]-[11].

In order to be compliant with IEC harmonic injection standards and also achieve high power factor operation, non-isolated three-phase mains interface concepts well suited for semi- or ultra-fast EV chargers are analysed and proposed in this paper (cf. Fig. 2). Aiming for high power capability and/or power efficiency EV systems, the circuit of conventional unidirectional CSRs are modified. As shown in Section II, multilevel CSRs appropriate for high power density EV chargers can be constructed by replacing the fast-switched semiconductors and output inductors of conventional CSRs with several modular circuits connected in parallel and operating with phase-shifted PWM. Simulation results of the proposed three-phase CSRs with a five-level configuration are presented. The converter specifications considered in the analyses are shown in Tab. I. Additionally, in Section III, bidirectional multilevel CSRs are proposed. Finally, in Section IV, a hardware prototype of a three-phase five-level six-switch buck-type PFC is tested to attest the feasibility of this multilevel CSR.

II. EV BATTERY CHARGING EMPLOYING MODULAR CURRENT SOURCE RECTIFIERS

In this section, five multilevel CSRs based on known unidirectional PFC topologies, such as the six-switch buck-type PFC rectifier [8]-[12] (cf. Fig. 2(a)), the Hybrid-Switch Active 3rd Harmonic Injection Rectifier (H3R) with a DC-DC buck-type converter [13] (cf. Fig. 2(b)), and the SWISS rectifier (SR) I [14], are proposed. The multilevel CSRs depicted in Fig. 2(d) and Fig. 3

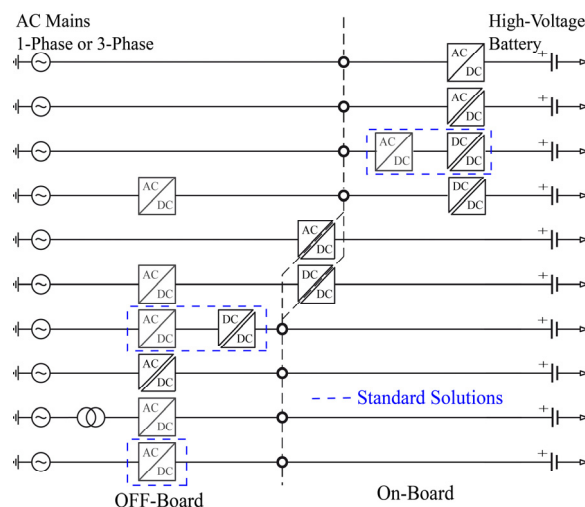


Fig. 1. Power electronic converter topologies for EV charging systems [5].

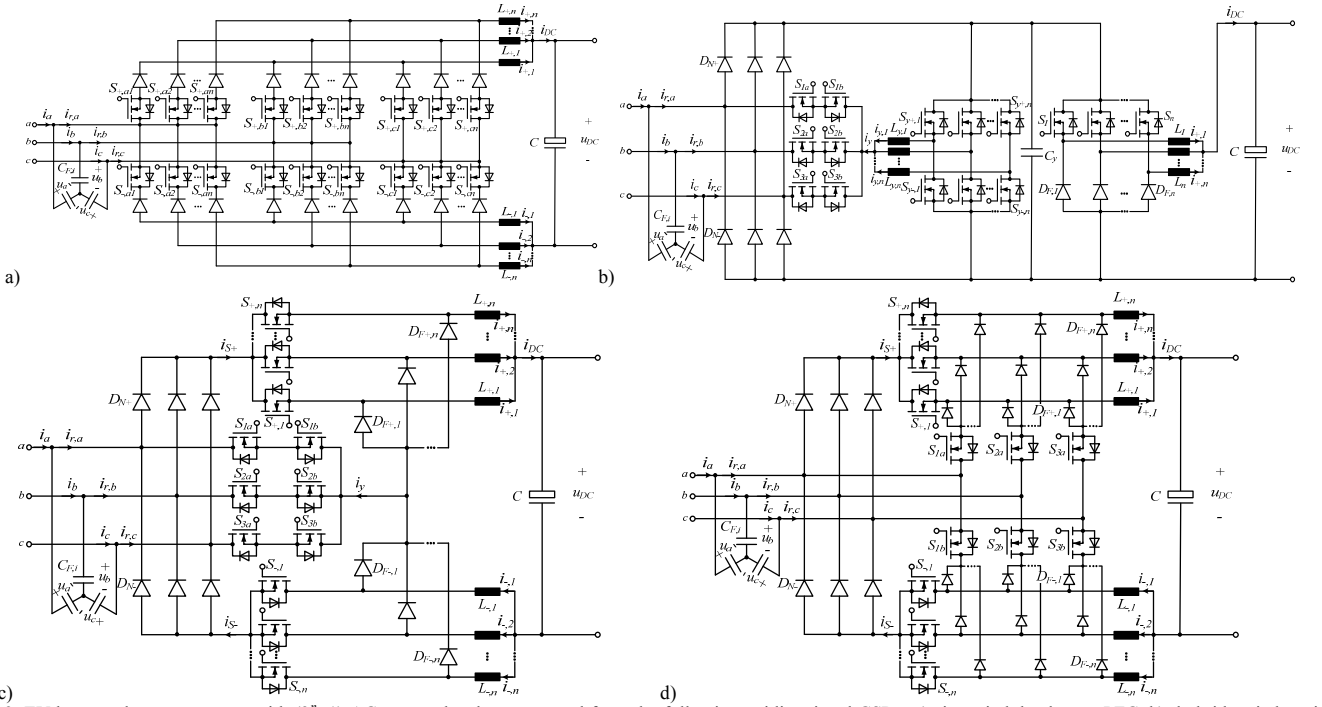


Fig. 2. EV battery charger concepts with (2^n+1) AC current levels constructed from the following unidirectional CSRs: a) six-switch buck-type PFC, b) hybrid-switch active 3^{rd} harmonic current injection rectifier and a DC-DC buck-type converter, c) SWISS rectifier I, and d) SWISS rectifier II.

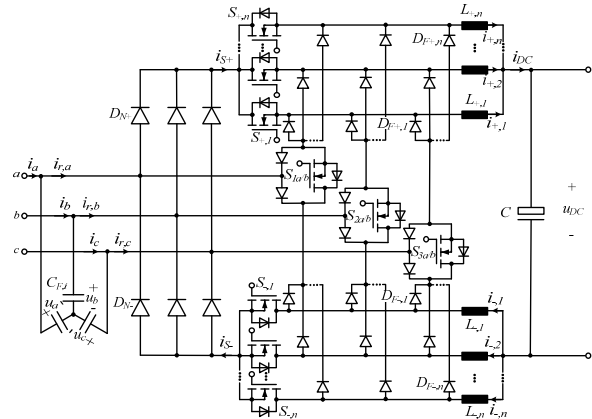


Fig. 3. Three-phase (2^n+1) -level hybrid-switch active 3^{rd} harmonic current injection rectifier based on the SR technology, referred to here as SR III.

TABLE I. Three-phase multilevel buck-type rectifier specifications.

Input phase voltage $u_{a,b,c}$ rms value	110 V
Mains frequency f_N	50 Hz
Switching frequency f_p	36 kHz
Rated output power P_0	12 kW
Output capacitor C	470 μF
DC inductor L	100 μH
Input Filter $L_{F,i}$ and $C_{F,i}$	100 $\mu\text{H}/6 \mu\text{F}$

are derived from the SR I depicted in Fig. 2(c), where different circuit implementations of the four-quadrant switches of the current injection network $S_{1a/b}$, $S_{2a/b}$ and $S_{3a/b}$ can be observed.

By analyzing the CSRs depicted in Fig. 2 and 3, it can be observed that the fast-switched semiconductors and the DC-link inductors of the conventional CSRs are assembled with n parallel connections of those circuits. The operation of these modular subcircuits with phase-shifted PWMs is advantageous as the CSRs face cancellation of current harmonics having pulse frequency, f_p ,

across the passive filters; i.e. for a five-level CSR, constructed with two paralleled circuits ($n = 2$), the first current harmonic occurs at double pulse frequency $2f_p$. Therefore, as the cut-off frequency of the passive filters can be shifted to higher frequencies, their sizes can be reduced. In addition, as the total DC-link current is distributed to several fast-switched devices, better efficiency, due to the lower conduction and switching losses, is achievable.

As the multilevel CSR can be operated with only a single circuit of the modular arrangements, i.e. it operates as a conventional CSR, the system can be designed to tolerate a faulty subcircuit. In this case, the system could be re-activated without the faulty circuit at the cost of reducing the CSR power capability and of increasing the current and voltage ripples at the input and output terminals. This interesting feature not only makes the CSR more reliable, but it could also be used to enhance the power efficiency of the systems for partial load operation. For instance, for low power levels it could make sense to only activate a few subcircuits, since the equivalent system would operate at a relatively higher power level and therefore with a higher efficiency than a multiple parallel system equally sharing the power [15].

A. Three-Phase Multilevel Six-Switch Buck-Type Rectifier

Fig. 2(a) presents a CSR featuring $(2^n + 1)$ current levels at the AC terminals, where n represents the number of paralleled subcircuits used to assemble the modular system. This multilevel CSR has already been studied in [16]. As for the conventional six-switch buck-type PFC, the output voltage range of the converter is limited by the minimal value of the six-pulse diode bridge output voltage as given by

$$u_{DC} < \sqrt{\frac{3}{2}} u_{N,l-l,rms} \quad (1)$$

where, u_{DC} is the output voltage of the CSR and $u_{N,l-l,rms}$ is the line-to-line rms value of the input voltage.

TABLE II: Applied duty cycle for the multilevel six-switch buck-type PFC rectifier. (cf. Fig. 4 and Eq. (2)) [8].

Sector	$\delta_{eff,a}$	$\delta_{eff,b}$	$\delta_{eff,c}$
1, 7	δ_a	$1 - \delta_c + t_d$	δ_c
2, 8	δ_a	$1 - \delta_a + t_d$	δ_c
3, 9	$1 - \delta_b + t_d$	δ_b	δ_c
4, 10	$1 - \delta_c + t_d$	δ_b	δ_c
5, 11	δ_a	δ_b	$1 - \delta_a + t_d$
6, 12	δ_a	δ_b	$1 - \delta_b + t_d$

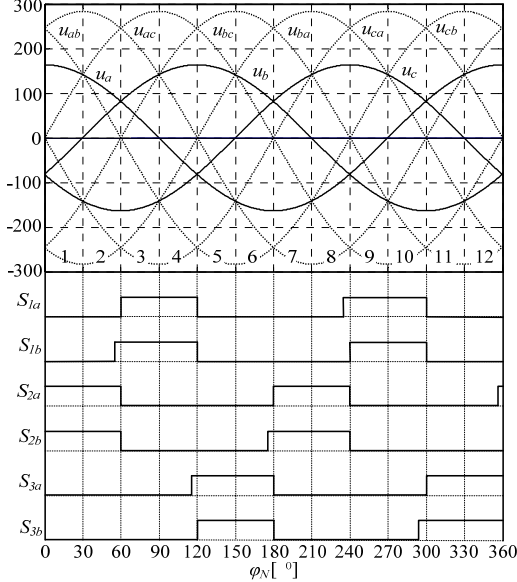


Fig. 4. Mains sectors 1 to 12 defined by the different relations of the instantaneous values of the mains phase voltages $u_{a,b,c}$ and respective gate signals of the third harmonic injection circuit switches providing the injection current logic and the required uninterrupted current path [13].

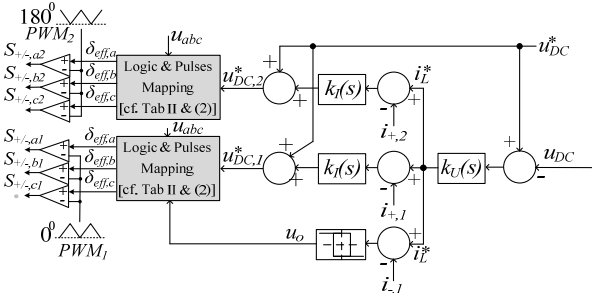


Fig. 5. Block diagrams of the phase-shifted PWM control.

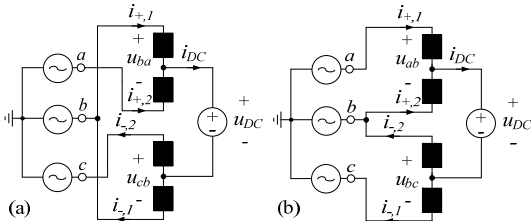


Fig. 6. Voltage applied to the DC-link inductors during the freewheeling state of (a) structure 1, and (b) structure 2.

An alternative to the three-phase CSR depicted in Fig. 2(a), having the number of active switches halved, would be the multilevel converter derived from the three-switch buck-type PFC studied in [17]. For this topology, a higher utilization of each switch is achieved, but at the cost of doubling the number of diodes. Unfortunately, also a higher number of components are involved in the current conduction path, generating higher

conduction losses than the aforementioned multilevel assembled with the six-switch CSR.

In this work, the modulation scheme for the unidirectional CSR presented in [8], is considered. This incorporates a short interval t_d during which switch on-times overlap, always guaranteeing a current path for an impressed DC current, where the duty ratios $\delta_{a,b,c}$ for the bridge legs are set according to

$$\delta_i = \frac{u_{DC}^*}{u_a^2 + u_b^2 + u_c^2} |u_i| \quad (2)$$

where u_{DC}^* is the reference rectifier output voltage and $i = \{a,b,c\}$. In this modulation strategy the transistors corresponding to the same phase-leg are switched at the same time, with duty cycles corresponding to the values presented in Tab. II. Accordingly, the active switch and diode (half of the leg) that conducts is determined by the input voltages. The $(2^n + 1)$ -pulse characteristic of the input current is obtained by equally phase-shifting the switches command of each converter phase-leg with the phase displacement of $\Delta\phi = 360^\circ/n$ within a pulse period.

Fig. 5 presents a suitable feedback PWM control scheme for a five-level CSR which is able to regulate the output voltage of the converter u_{DC} and AC currents by conditioning the variable $u_{DC,1/2}^*$ used in the modulator according to the current control of the DC-link currents. Therein, a slow outer control loop is used to regulate the output voltage to a constant reference voltage u_{DC}^* and to generate the reference value i_L^* for the two fast inner DC current loops of the upper modularized DC-link inductors $L_{+,1/2}$, $i_{+,1}$ and $i_{+,2}$. The current controllers produce the output voltage reference values, $u_{DC,1}^*$ and $u_{DC,2}^*$, which are utilized in the calculation of the active switches relative on-times $\delta_{eff,abc}$ of the parallel CSR-stages (cf. (2) and Tab. II). These will provide proper portioning of the DC-link current among the inductors $L_{+,1/2}$, i.e. $i_{+,1} = i_{+,2} = i_{DC}/2$.

In order to achieve a symmetric distribution of the currents in the DC-link inductors $L_{-,1/2}$, a tolerance band logic obtained by comparing $i_{-,1}$ and the current reference i_L^* is used to guide the utilization of the calculated freewheeling states (zero vectors) of the paralleled subcircuits. For an arbitrary sector, the freewheeling states apply different line-to-line voltages at the upper and bottom DC-link inductor terminals. This characteristic is shown in Fig. 6 for the first mains sector. Therefore, in case the current of the bottom inductor deviates from the reference value, the duration of the freewheeling state of a structure can be modified for a short time to force the current $i_{-,1}$ (and hence $i_{-,2}$) to be equal to $i_{DC}/2$.

Fig. 7 presents simulated characteristic waveforms of the conventional six-switch buck-type PFC (cf. Fig. 7(a)) and of a five-level CSR (cf. Fig. 7(b)). These systems are considered to be operating under rated power with converter specification given in Tab. I. For the multilevel CSR, in order to maintain the relative amplitude of the current ripple in each inductor $L_{+/-,n}$ of the bridge-legs, $\Delta i L_{+/-,n} / i_{+,avg}$, similar to the one obtained across the inductor L of the conventional CSR, $\Delta i L / i_{DC,avg}$, the relation $L_{+/-,n} = nL$ is considered. In this way, both systems have comparable total amounts of energy stored in their inductors.

The simulation results depicted in Fig. 7 demonstrate that in the studied CSRs the line currents $i_{a,b,c}$ can effectively follow the sinusoidal input phase voltages $u_{a,b,c}$. As expected, the five-level CSR features lower current ripples at the input and output terminals than the conventional system when passive filters of same total volume are considered. Note that, if the analysis was considering the CSRs operating with fixed maximum voltage or current ripple at the input and output filters, the passive filter sizes of the five-level CSR would be smaller than those of the conventional system.

B. Three-Phase Multilevel Hybrid 3rd Harmonic Current Injection Rectifier + DC-DC Buck-Type Converter

Another interesting multilevel three-phase buck-type PFC rectifier is depicted in Fig. 2(b). This circuit combines an active current injection electrolytic capacitor-less converter (front-end) with a series connected DC-DC buck-type converter (back-end) [13]. This H3R implementation is very attractive as few active switches in the main current path exist (only the power transistors of the back-end converter), leading to low conduction losses, i.e. in particular at high output voltages with the back-end converter operating with short freewheeling intervals. Additionally, the components in the current injection circuit require relatively low current rating devices, i.e. the maximum value of the flowing

current is rated half the amplitude of the sinusoidal input current. Advantageously, the negative output voltage terminal is always connected to the mains via a diode of the rectifier. Therefore, no output common-mode (CM) voltage with switching frequency is generated. The implementation effort of the CM EMI filter can, thus be reduced as only the parasitic capacitors of the power semiconductors lead to high-frequency CM noise currents.

For the system presented in Fig. 2(b), the modulation of the current injection circuit $S_{123,a/b}$ could be performed at low frequency (twice the input frequency, with two 60° conduction intervals within a grid period), following the rectifier input voltages $u_{a,b,c}$ in such a way that the active current injection always occurs into only one mains phase as presented in Tab. III. Due to the requirement of

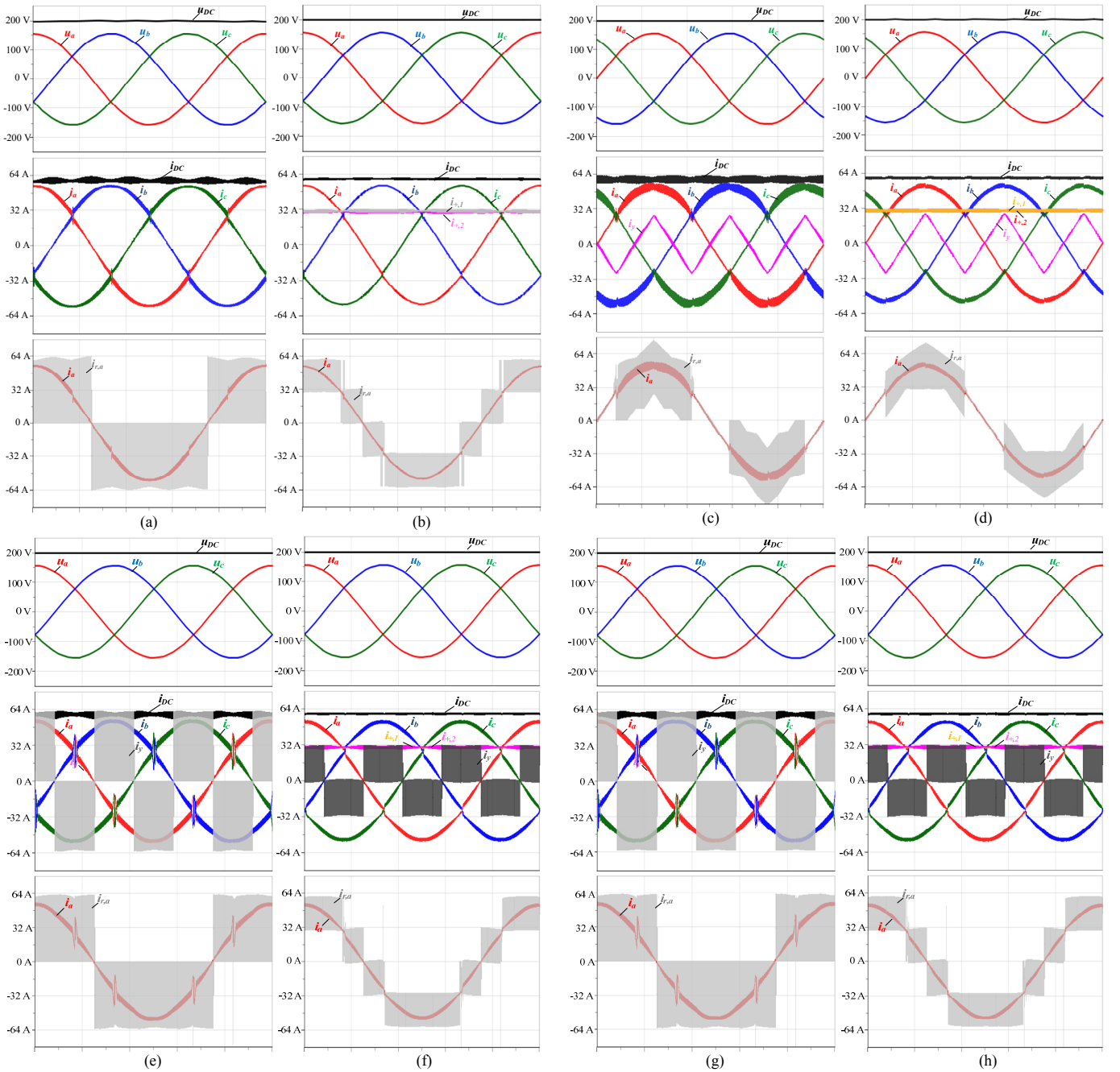


Fig. 7. Simulation results for the studied multilevel CSRs: (a) Conventional and (b) five-level six-switch buck-type rectifier; (c) conventional and (d) five-level H3R + DC-DC buck-type converter; (e) conventional and (f) five-level SWISS rectifier I; and (g) conventional and (h) five-level SWISS rectifier II.

TABLE III. Modulation of the current injection circuit of a H3R (cf. Fig. 4).

Sector	S_{y1a}	S_{y1b}	S_{y2a}	S_{y2b}	S_{y3a}	S_{y3b}
0° - 60°	0	0	1	1	0	0
60° - 120°	1	1	0	0	0	0
120° - 180°	0	0	0	0	1	1
180° - 240°	0	0	1	1	0	0
240° - 300°	1	1	0	0	0	0
300° - 360°	0	0	0	0	1	1

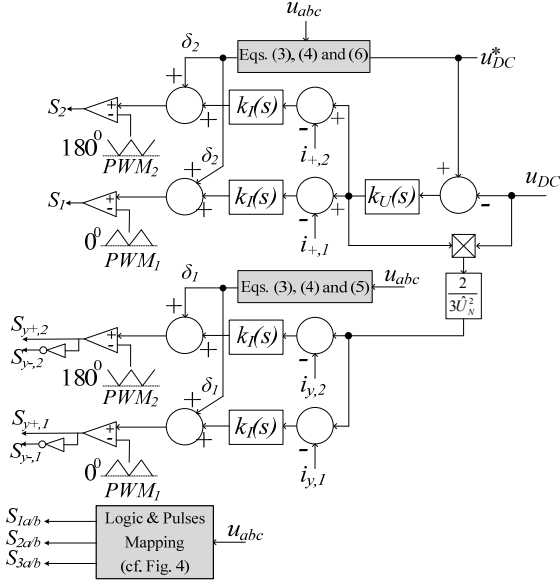


Fig. 8. Block diagrams of the phase-shifted PWM control appropriate for operation of the five-level H3R + DC-DC buck-type converter.

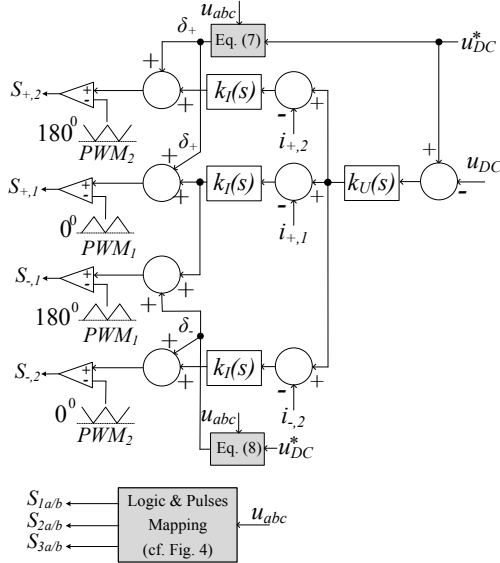


Fig. 9. Block diagrams of a phase-shifted PWM control appropriate for operation of the SWISS rectifiers.

uninterrupted current flow through the modular inductors $L_{y,n}$, while still allowing a dead-time among the switches, $S_{123,a/b}$, to prevent short-circuits between the individual phases, the modulation depicted in Fig. 4 is implemented.

For sinusoidal input currents, the duty cycle δ_1 for the fast-switched devices of the current injection circuit, $S_{y+/-,n}$, can be determined with

$$u_{pos} = \max(u_a, u_b, u_c) \quad (3)$$

$$u_{neg} = \min(u_a, u_b, u_c) \quad (4)$$

$$\delta_1 = \frac{-(u_{pos} + 2u_{neg})}{u_{pos} - u_{neg}} \quad (5)$$

For the back-end converter the duty cycle δ_2 is given by

$$\delta_2 = \frac{u_{DC}^*}{u_{pos} - u_{neg}} \quad (6)$$

A possible implementation of a control scheme for the studied multilevel H3R is shown in Fig. 8, and consists of two control loops: one for the DC-DC converter, corresponding to the constant-power load and a second for the current injection circuit, controlling the voltage applied across $L_{y,n}$, thus regulating the current injected into the mains.

In Fig. 7 simulated waveforms of the conventional H3R + DC-DC converter [13] (cf. Fig. 7(c)) and of a five-level arrangement of this rectifier technology (cf. Fig. 7(d)) are shown. As for the previous rectifier concept, the analysis considers these systems to be operating at rated power with the converter specification given in Tab. I. The total volumes of the passive elements are the same for the conventional and for the multilevel modular systems.

The simulation results shown in Fig. 7 demonstrate that in both CSRs the line currents $i_{a,b,c}$ can effectively follow the sinusoidal input phase voltages $u_{a,b,c}$. As expected, the five-level CSR features lower current ripples at the input and output terminals than the conventional circuit.

C. Three-Phase Multilevel SWISS Rectifier Technology

The circuit schematic depicted in Fig. 2(c), also referred to here as the SWISS Rectifier I (SRI) [14], is another three-phase multilevel CSR which is based on a 3rd harmonic current injection circuit. Other configurations of a multilevel SWISS rectifier are depicted in Fig. 2(d) (SRII) and Fig. 3 (SRIII), where the current injection circuits are assembled from conventional three-phase buck-type PFC rectifiers.

The output voltage range of the SRs is limited by the minimal value of the six-pulse diode bridge output voltage, given by (1) and is therefore identical to the output voltage range for the CSRs shown in Fig. 2(a). Additionally, the current and voltage stresses across the input and output passive filters are similar.

For the SRs, the currents in the positive and negative active switches, i_{S+} and i_{S-} , are formed proportionally to the two phase voltages involved in the formation of the output voltage of the diode bridge, D_{N+} and D_{N-} . The difference between i_{S+} and i_{S-} is fed back into the grid phase with the currently smallest absolute voltage value via a current injection network $S_{123,a/b}$, formed differently in the studied SRs. In this way, PFC operation and controlled output voltage, u_{DC}^* , can be achieved by controlling $S_{+,n}$ and $S_{-,n}$ with duty cycles, δ_+ and δ_- , reliant on the instantaneous values of the input voltage, $u_{a,b,c}$, and the amplitude of the grid phase voltages \hat{U}_N ,

$$\delta_+ = \frac{2 u_{DC}^*}{3 \hat{U}_N^2} \cdot \max(u_a, u_b, u_c) \quad (7)$$

$$\delta_- = \frac{2 u_{DC}^*}{3 \hat{U}_N^2} \cdot |\min(u_a, u_b, u_c)| \quad (8)$$

The modulation of the current injection network is performed at low frequency, following the rectifier input voltages $u_{a,b,c}$ in such a way that the active current injection always occurs into only one grid phase as presented in Tab. III. In order to achieve low conduction losses, semiconductors with low forward voltage drop for the devices $D_{N+/-}$ and $S_{1a/b}$, $S_{2a/b}$, and $S_{3a/b}$ can be selected. Note that the injection switches of the SRI need to be gated with dead time among phases, which would be a problem when $i_y \neq 0$. In

order to solve this issue, the injection switches could be operated with the commutation strategy shown in Fig. 4. On the other hand, the SRII and SRIII are protected against phase-leg shoot-through, but a short interval t_d during a switch transition where the switch on-times overlap is used to guarantee the required path for the partial impressed DC current.

When comparing standard SRs ($n = 1$), the SRII depicted in Fig. 2(d), displays similar total switching losses as the SRI and SRIII, but has lower conduction losses during the current injection states, where only four devices conduct the DC current, i_{DC} . For the SRI and SRIII, during the current injection states there will always be five devices carrying i_{DC} . During the freewheeling state of the SRs, i_{DC} circulates through only two devices in the SRI, while for the SRIII and SRII the current flows through three and four semiconductors, respectively.

Fig. 9 shows a possible implementation of a feedback control scheme for the five-level SRs. This PWM control strategy comprises a superimposed output voltage controller $K_U(s)$ and subordinate output current controllers $K_I(s)$. Finally, feed-forward loops add the normalized modulation functions defined by the positive and negative diode bridge output voltage and the system output voltage reference u_{DC}^* to the DC current controllers.

In Fig. 7(e)-(f) and 7(g)-(h) simulation results of the conventional and five-level SRI and SRII are shown, respectively. As for the previous rectifier concept, the analysis considers these systems operating at rated power with the converter specification given in Tab. I. The total volumes of the passive elements are the same for the conventional and the multilevel modular systems. As can be observed, the results demonstrate that the line currents $i_{a,b,c}$ can effectively follow the sinusoidal input phase voltages $u_{a,b,c}$, attesting the feasibility of the SWISS rectifiers and PWM control method. Additionally, as can be clearly noted in Fig. 7(e)-(f), another advantage of the five-level SRs is the smaller injection current i_y , amplitude which leads to lower conduction losses in the injection circuit semiconductors when compared to the conventional systems.

III. BIDIRECTIONAL MODULAR MULTILEVEL CURRENT SOURCE RECTIFIERS

In Fig. 10 bidirectional modular multilevel buck-type PFC rectifier topologies are presented, based on the extension of some unidirectional converters depicted in Fig. 2. These systems have similar operating characteristics to the unidirectional converters from which they are derived. Another interesting bidirectional topology, known as multilevel inverting-link CSR is shown in Fig. 11(a) (in a five-level CSR configuration) [19].

IV. HARDWARE DEMONSTRATOR

A laboratory prototype of the three-phase five-level inverting-link CSR shown in Fig. 11(a) has been tested. This CSR hardware has a power capability of 2.5 kW and can be seen in Fig. 11(b). As can be noticed, this system implements inter-phase transformers, T_{i1} and T_{i2} , paralleling the two unidirectional six-switch CSRs. It is important to point out that the subcircuits of the other multilevel converters depicted in Fig. 2, 3 and 10 can also be connected in parallel association in a similar way by using inter-phase transformers and a single inductor as shown in Fig. 11(a). The advantages of the use of these transformers over conventional inductors, as shown in Fig. 2, have been studied in [18].

Fig. 11(c) and 11(d) show the main experimental results of the multilevel CSR operating as a unidirectional three-phase five-level six-switch buck-type PFC (with inverting-link circuit switches kept turned off) with a $u_{a/b/c} = 110$ V_{rms} (60 Hz) mains and $u_{DC} = 200$ V

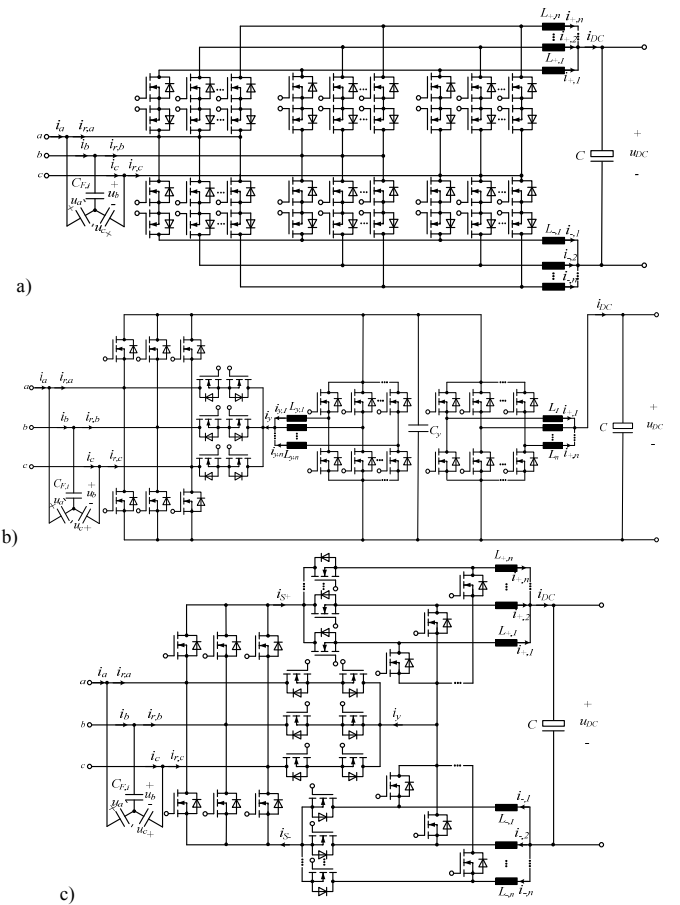


Fig. 10. Bidirectional EV battery charger concepts with (2^n+1) AC current levels constructed from the following unidirectional CSRs: a) six-switch buck-type PFC, b) hybrid-switch active 3rd harmonic current injection rectifier and a DC-DC buck-type converter, c) SWISS rectifier I.

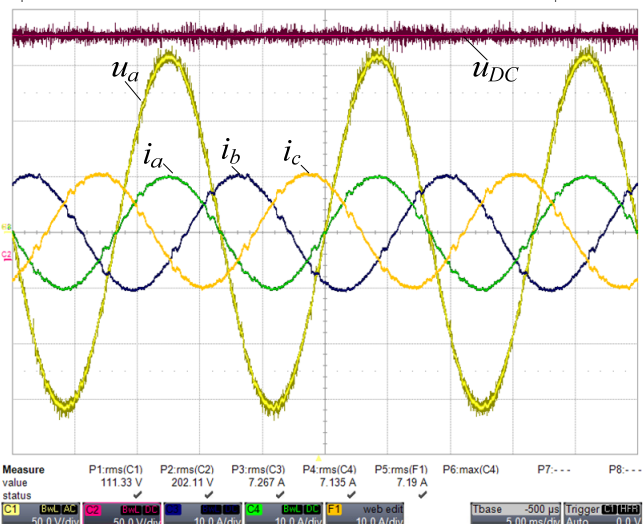
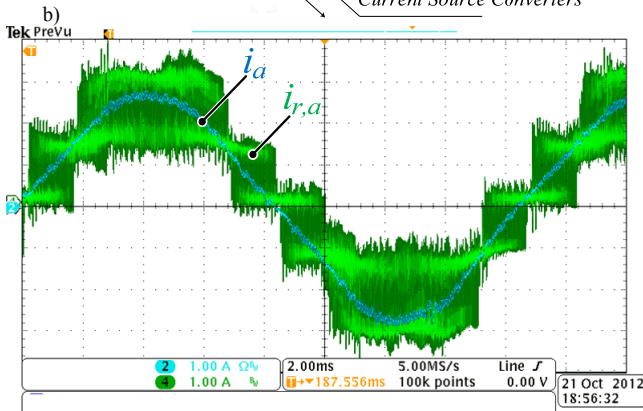
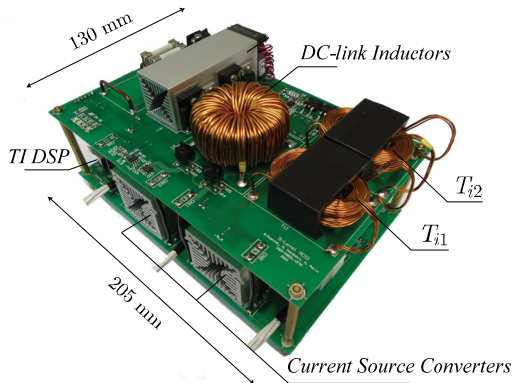
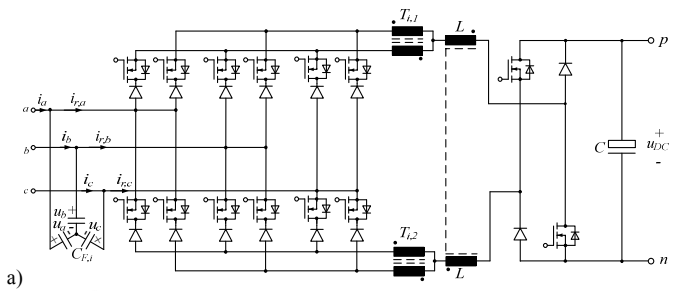
output voltage. As can be seen in Fig. 11(c), the input terminal current $i_{r,a}$ features five levels and generates a sinusoidal line current, i_a , after the AC filter. Additionally, as can be observed in Fig. 11(d), the line currents $i_{a,b,c}$ can effectively follow the sinusoidal input phase voltage u_a , while regulating the output voltage u_{DC} . Accordingly, the experimental results attest the feasibility of the studied converter and PWM control method.

V. CONCLUSION

This paper proposes three-phase multilevel high power factor mains interfaces based on current source converters which are appropriate not only for high power EV battery charging systems, but also for power supplies for telecommunication, DC distribution systems, and variable speed AC drives. The characteristics of the presented rectifier systems, including the principles of operation, modulation strategy, and suitable control structures, have been summarized. The feasibility of one multilevel converter was demonstrated by means of a hardware prototype.

REFERENCES

- [1] J. J. Chen, F.-C. Yang, C.-C. Lai, Y.-S. Hwang and R.-G. Lee, "A High Efficiency Multimode Li-Ion Battery Charger with Variable Current Source and Controlling Previous Stage Supply Voltage," *IEEE Trans. Ind. Elec.*, vol. 56(7), pp. 2469-2478, 2009.
- [2] M. Chen and G. Rincon-Mora, "Accurate, Compact, and Power-Efficient Li-Ion battery Charger Circuit," *IEEE Trans. Circ. Sys. II: Expr. Briefs*, vol. 53(11), pp. 1180-1184, 2006.



d) Implemented 2.5 kW five-level inverting-link six-switch PFC rectifier; b) hardware prototype; c) phase a terminal current with five-level feature and filtered line current; and d) output voltage u_{DC} , input currents, $i_{a,b,c}$, and phase a voltage, u_a . Note that the current i_c was calculated from the measured i_a and i_b .

- [3] R. Gitzendanner, F. Puglia, C. Martin, D. Carmen, E. Jones and S. Eaves, "High Power and High Energy Lithium-Ion Batteries for Underwater Vehicles," *J. Pow. Sources*, vol. 136, 2004.
- [4] B. Kennedy, D. Patterson and S. Camilleri, "Use of Lithium-Ion Batteries in Electric Vehicles," *J. Pow. Sources*, vol. 90, 2000.
- [5] T. B. Soeiro, T. Friedli, and J. W. Kolar, "Three-phase high power factor mains interface concepts for electric vehicle battery charging systems," in *Proc. 26th IEEE Appl. Power Electron. Conf. Exp.*, pp. 2603–2610, Feb. 5–9, 2012.
- [6] D. Aggeler, F. Canales, H. Zelaya, A. Coccia, N. Butcher, and O. Apeldoorn, "Ultra-Fast DC-Charger Infrastructures for EV-Mobility and Future Smart Grids", *Proc. ISGT*, 2010.
- [7] A. Kuperman, U. Levy, J. Goren, A. Zafranski and A. Savernin, "High Power Li-Ion Battery Charger for Electric Vehicle", *Proc. Conf. Workshop Compatib. and Power Electron. (CPE)*, 2011.
- [8] A. Stupar, T. Friedli, J. Miniböck, and J.W. Kolar, "Towards a 99% efficient three-phase buck-type pfc rectifier for 400 v dc distribution systems", *IEEE Trans. on Power Electr.*, Apr. 2012.
- [9] Fan Xu; Ben Guo; Tolbert, L.M.; Wang, F.; Blalock, B.J., "Design and performance of an all-SiC three-phase buck rectifier for high efficiency data center power supplies," *Energy Conversion Congress and Exposition (ECCE), 2012 IEEE*, vol., no., pp.2927,2933, 15-20 Sept. 2012.
- [10] Cuzner, R.; Drews, D.; Venkataramanan, G., "Power density and efficiency of system compatible, sine-wave input/output drives," *Energy Conversion Congress and Exposition (ECCE), 2012 IEEE*, vol., no., pp.4561,4568, 15-20 Sept. 2012.
- [11] Fan Xu; Ben Guo; Tolbert, L.M.; Wang, F.; Blalock, B.J., "Evaluation of SiC MOSFETs for a high efficiency three-phase buck rectifier," *Applied Power Electronics Conference and Exposition (APEC), 2012 Twenty-Seventh Annual IEEE*, vol., no., pp.1762,1769, 5-9 Feb. 2012.
- [12] T. Callaway, J. Cass, R. Burgos, F. Wang, D. Boroyevich, "Three-phase ac buck rectifier using normally-on sic jfets at a 150 kHz switching frequency", in *Proc. 38th IEEE Power Electron. Specialists Conf. (PESC 2007)*, Jun. 2007.
- [13] T. Soeiro, F. Vancu and J. W. Kolar, "Hybrid active 3rd harmonic current injection mains interface concept for dc distribution systems," *IEEE Trans. on Power Electron.*, Jan. 2012.
- [14] T. Soeiro, T. Friedli and J. W. Kolar, "Design and implementation of a three-phase buck-type third harmonic current injection pfc rectifier (swiss rectifier)," *IEEE Trans. on Power Electr.*, 2013.
- [15] J. W. Kolar, F. Krismer, Y. Lobsinger, J. Muhlethaler, T. Nussbaumer, J. Minibock, "Extreme efficiency power electronics," in *Proc. of the Int. Conf. Integ. Power Electr. Systems (CIPS)*, March, 2012.
- [16] B. S. Dupczak, A. Perin, and M. L. Heldwein, "Space vector modulation strategy applied to interphase transformers-based five level current source inverters", *Trans. on Power Electr.*, 2012.
- [17] M. Baumann, and J. W. Kolar, "Dc side current balancing of two parallel connected interleaved three-phase three-switch buck-type unity power factor pwm rectifier systems," in *Proc. of the 8th Europ. Power Quality Conf. (PCIM)*, May. 2002.
- [18] B. Cougo, T. Friedli, D. o. Boillat, and J. W. Kolar, "Comparative evaluation of individual and coupled inductor arrangements for input filters of pv inverter systems," in *Proc. of the Int. Conf. Integ. Power Electr. Systems (CIPS)*, March, 2012.
- [19] T. Soeiro, M. Ortmann and M. L. Heldwein, "Three-phase five-level bidirectional buck- + boost-type pfc converter for dc distribution systems", *IEEE Int. Conf. on Ind. Techn. (ICIT)*, Feb., 2013.